The effect of oblique convergence on temperature in subduction zones: insights from 3D numerical modelling

Alexis Plunder, Cédric Thieulot and Douwe van Hinsbergen
Utrecht University, Department of Earth Sciences

Universiteit Utrecht

1. Introduction

In subduction zone the geotherm is thought to vary as a function of subduction rate and the age of the subducting lithosphere. Along a single subduction zone the rate of subduction can strongly vary due to changes in the angle between the trench and the plate convergence vector, namely the subduction obliquity. This phenomenon is observed all around the Pacific (Fig. 1; i.e. Marianna, Sunda-Sumatra, Aleutian…) and is supposed in the geological record of Turkey. However due to observed differences in subducting lithosphere age or lateral convergence rate in nature, the quantification of temperature variation due to obliquity is not obvious and need to be better constrained. In order to investigate this effect, 3D generic numerical models were carried out using the finite element code ELEFANT.

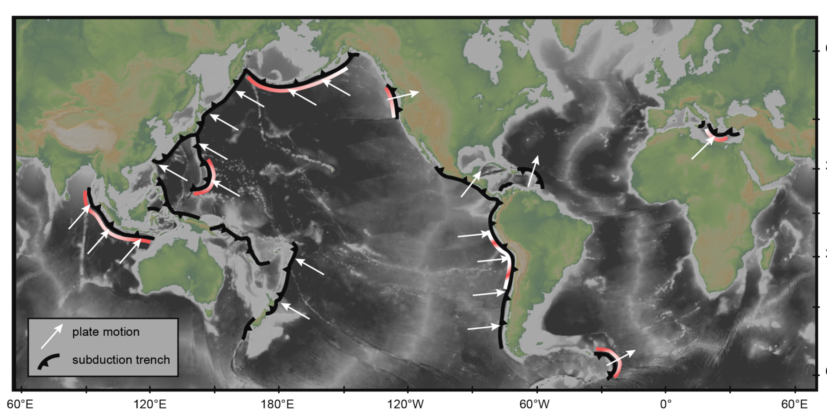

Figure 1: Plate motion at trenches from the NNR-MORVEL model [1]. Baselayer obtain with GeoMapApp (`http://www.geomapapp.org`) with topography and bathymetry from [2]

2. Setup and strategy

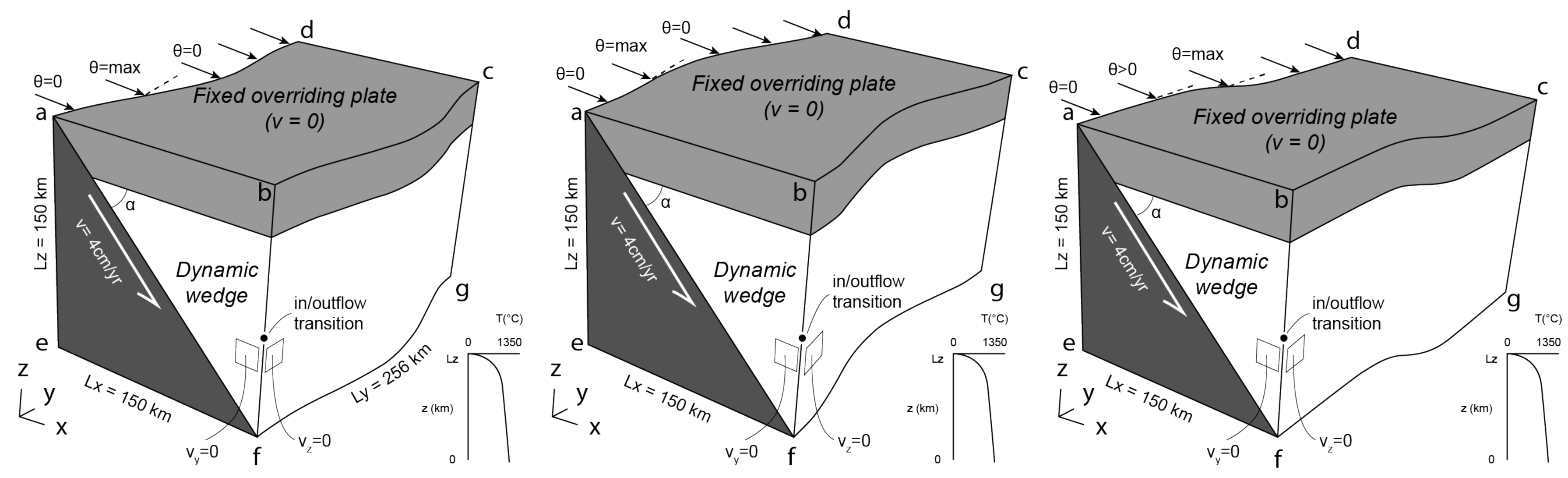

Figure 2: Setup of the numerical model.

We use the finite element code ELEFANT[3] to solve the mass, momentum and energy equations in three-dimensions:

$$\nabla \cdot \boldsymbol{v} = 0 \quad (1)$$

$$-\nabla P + \nabla \cdot (2\mu\dot{\varepsilon}) = \rho \boldsymbol{g} \quad (2)$$

$$\rho_0 c_p \left(\frac{\partial T}{\partial t} + \boldsymbol{v} \cdot \nabla T \right) = \nabla \cdot (k \nabla T) \quad (3)$$

Eqs.(1,2) are solved for a set of geometry and boundary condition. Then, the same $\boldsymbol{v}$ is used to solve Eq. (3) until steady state is reached (Fig 3). The geometry is prescribe by the means of a simple sine or arctangente function to describe a convex, concave or S-shaped subduction zone. The temperature is measured along the interface using tracers

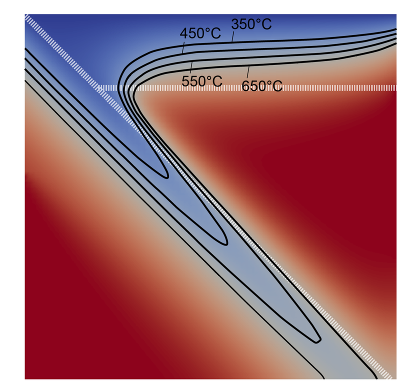

Figure 3: Thermal structure on the side of the modelling space after reaching steady-state

3. Results

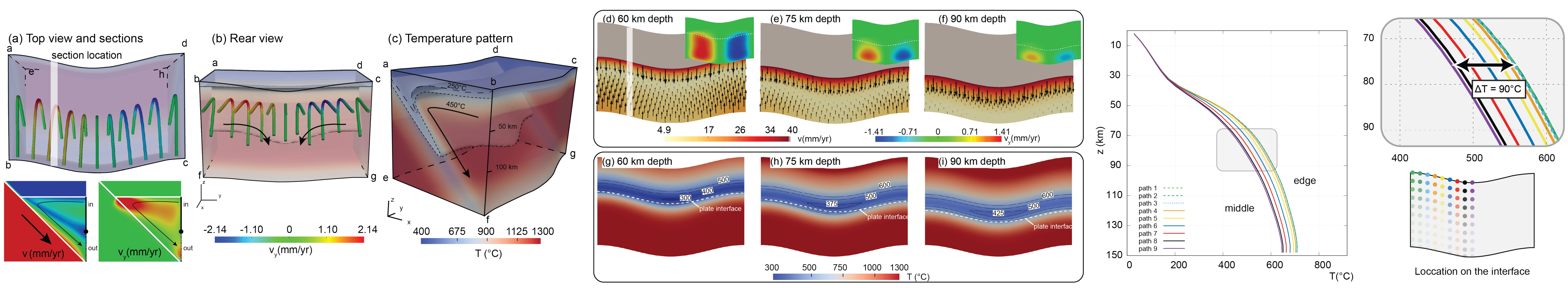

Figure 4: Compilation of plots for the reference model. (a) top view of the mantle flow and section of the velocity (both v and v_y) on the side of the model; (b) rear vie of the modling box showing the mantle flow and the shape of the 450°C isotherm; (c) temperature pattern in the model. Note the deflection of the 450°C isotherm; (d,e,f) Direction of the mantle flow at different depths and value of the v_y; (g,h,i) temperature pattern at different depth. Right pannel: Depth–Temperature path along the plate interface, close-up and location of the tracers.

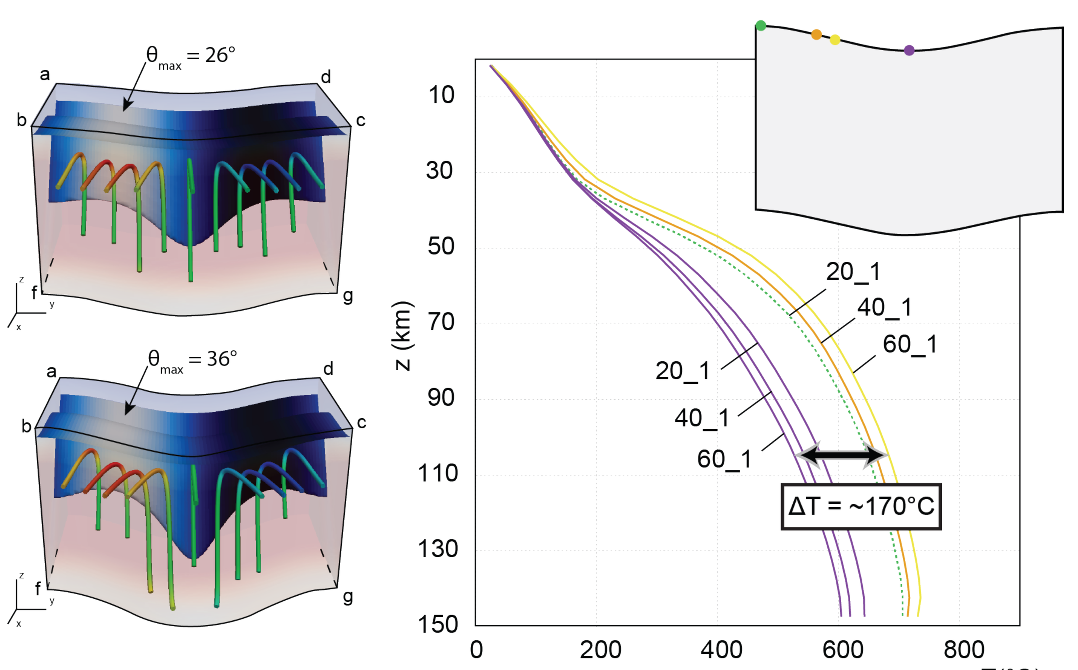

Figure 5: Mantle flow for different geometry and compilation of depth–temperature paths for the SIN-shaped models

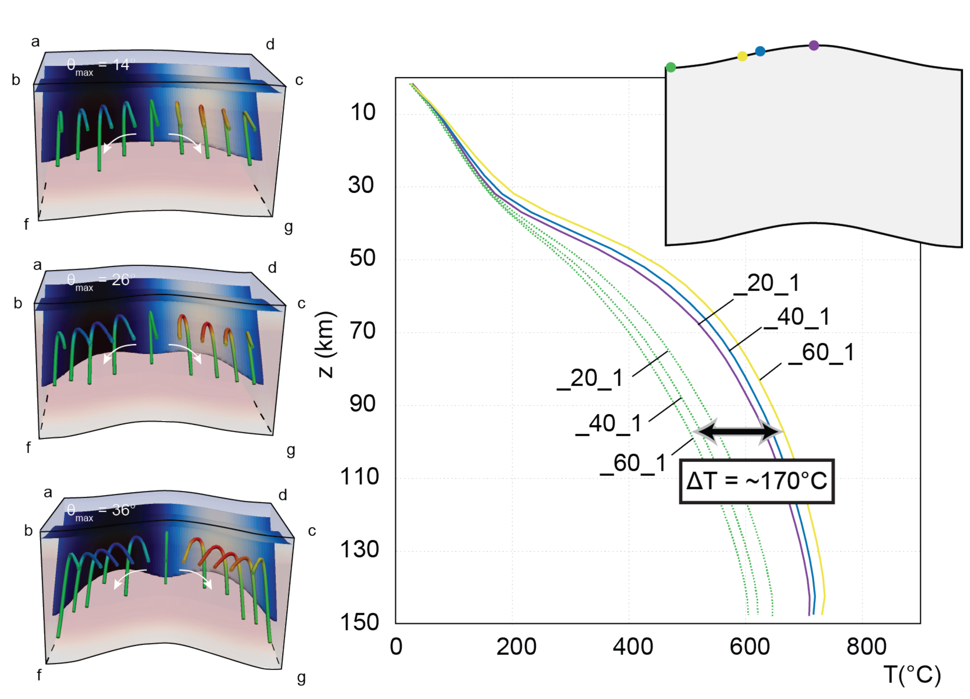

Figure 6: Mantle flow for different geometry and compilation of depth–temperature paths for the -SIN-shaped models

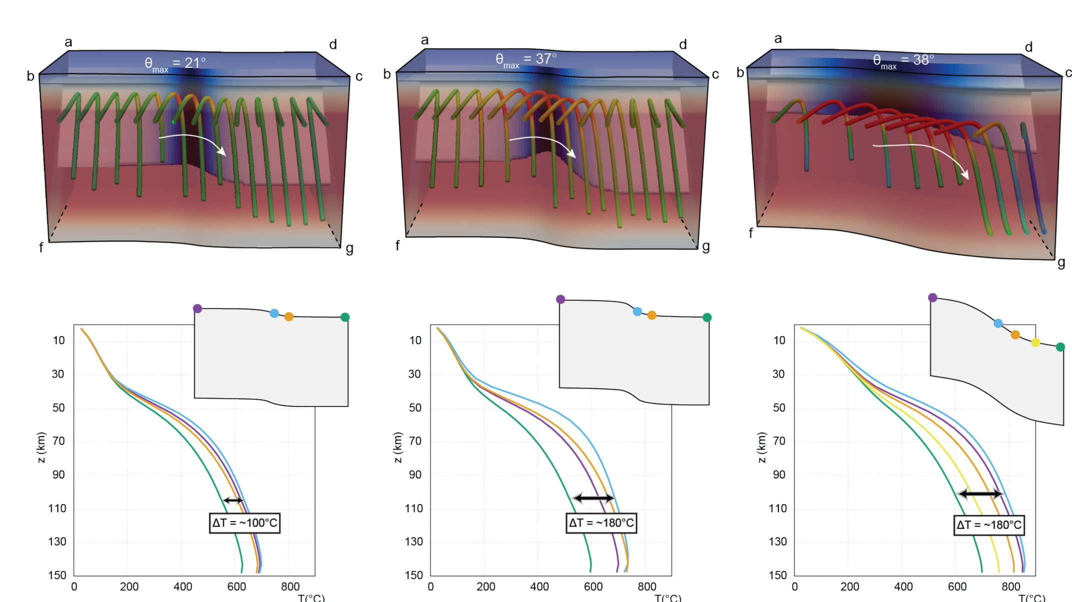

Figure 7: Mantle flow and compilation of depth–temperature paths for the S-shaped modeletate is different for model 40_05

4. Significance for subduction zones and future research

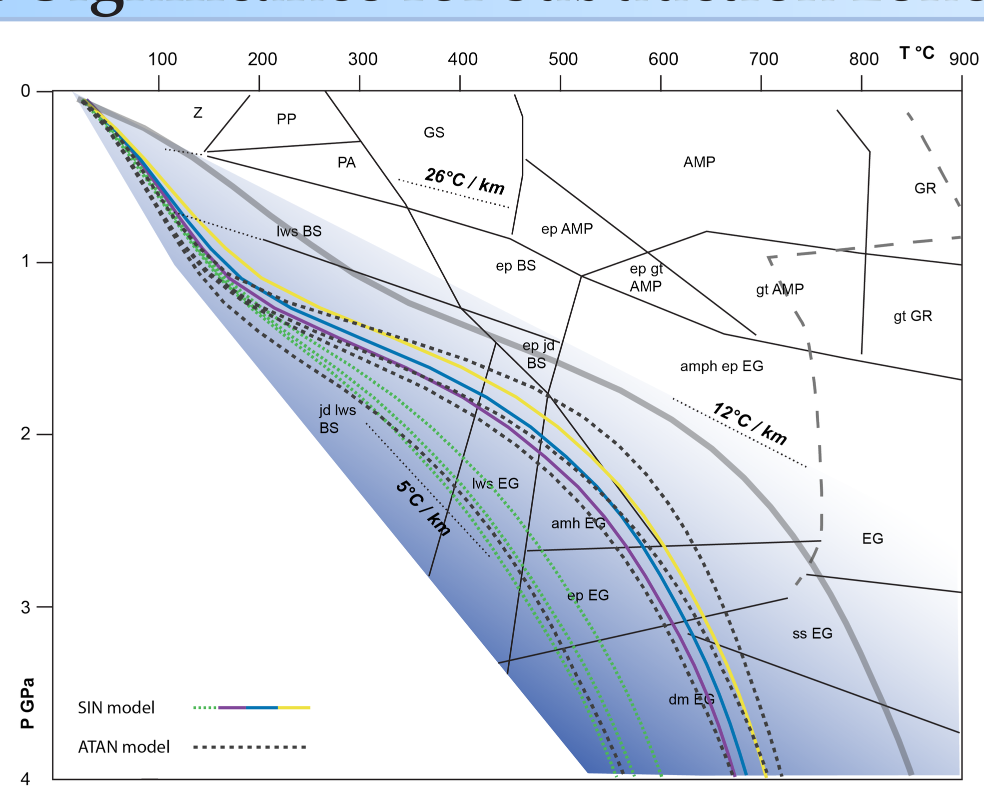

Figure 8: PT path of the differnet models plotted on a phase diagram for a MORB composition after [5].

The thermal regime in the model can be very different (with geotherm from 5 to 12°C/km) according to the prescribed geometry, with $\Delta T = 200°C$ from 50–70 km depth (Figs 4,5,6,7 & 8). Here the range of Temperature–Depth profile show that within the same subduction zone different PT regime can be encoutered. This has implication for the general undestanding of subduciton zone mechanism (such as mechanical coupling and related seismicity that is linked to temperature via dehydration reactions). These important effect might also be linked to the differences of magmatism (and amount of partial melting in the mantle wedge) along trenches, for example in south America. The effect of obliquity is more important that admitted as showed by our first order models. Tests performed with different velocity and/or slab dip show similar effects.

Future work:

1. Test with "real geometries" (i.e. slab dip and model domain; Marianna, South America)
2. More complex material (*i.e* crust and mantle)
3. Non-linear rheologies (ASPECT? Ptatin?)
4. Link with mantle tomography and implication for segmented slabs

Contact Information

Email alex.plunder@gmail.com
Address Dept. of Earth sciences. Heidelberglaan 2, 3584CS Utrecht, The Netherlands

A. P was funded throught the ERC starting grant SINK (306810) awarded to D.J.J. v.H.

References

[1] D. F. Argus, R. G. Gordon, and C. Demets. Geologically current motion of 56 plates relative to the no-net-rotation reference frame. *Geochemistry, Geophysics, Geosystems*, 12(11):1–13, 2011.

[2] W. B.F. Ryan, S. M. Carbotte, J. O. Coplan, S. O'Hara, A. Melkonian, R. Arko, R. A. Weissel, V. F. A. Goodwillie, F. Nitsche, J. Bonczkowski, and R. Zemsky. Global multi-resolution topography synthesis. *Geochemistry, Geophysics, Geosystems*, 10(3), 2009.

[3] C. Thieulot. ELEFANT: a user-friendly multipurpose geodynamics code. *Solid Earth*, 6:1949–2096, 2014.

[4] D. P. McKenzie. Speculations on the conséquences and causes of plate motions. *Geophys. J. Roy. Astron. Soc.*, 18(1608):1–32, 1969.

[5] B. R. Hacker, G. A. Abers, and S. M. Peacock. Subduction factory 1. Theoretical mineralogy, densities, seismic wave speeds, and H2O contents. *Journal of Geophysical Research*, 108(B1):2029, 2003.